Geologica Acta, Vol.14, Nº 2, June 2016, 139-154
DOI: 10.1344/GeologicaActa2016.14.2.4

geologica acta

Response of alluvial systems to Late Pleistocene climate changes recorded by environmental magnetism in the Añavieja Basin (Iberian Range, NE Spain)

B. OLIVA-URCIA[1,2] A. MUÑOZ[3] J.C. LARRASOAÑA[4,5] A. LUZÓN[3] A. PÉREZ[3] Á. GONZÁLEZ[3] Z. JIANG[6] Q. LIU[6,7] T. ROMÁN-BERDIEL[8]

[1]Instituto Pirenaico de Ecología, CSIC
Avda. Montañana 1005, 50059 Zaragoza, Spain

[2]Dpto. de Geología y Geoquímica, Universidad Autónoma de Madrid
Ciudad Universitaria de Cantoblanco, 28049 Madrid, Spain

[3]Dpto. Ciencias de la Tierra. Universidad de Zaragoza, Área de Estratigrafía
Pedro Cerbuna, 12, 50009 Zaragoza, Spain

[4]Instituto Geológico y Minero de España (IGME)
Manuel Lasala, 49, 50006 Zaragoza, Spain

[5]Institute of Earth Sciences Jaume Almera, ICTJA-CSIC
Solé i Sabarís s/n, 08028 Barcelona, Spain

[6]Paleomagnetism and Geochronology Laboratory, Institute of Geology and Geophysics, Chinesse Academy of Sciences
19 Beituchengxi Road, Chaoyang District, Beijing 100029, China

[7]Function Laboratory for Marine Geology, National Oceanography Laboratory
Qingdao 266061, China

[8]Dpto. Ciencias de la Tierra. Universidad de Zaragoza. Área de Geodinámica Interna
Pedro Cerbuna, 12, 50009 Zaragoza, Spain

ABSTRACT

Environmental magnetic proxies were analyzed in a relatively monotonous, ~25.3m thick alluvial sedimentary sequence drilled in the Añavieja Basin (NE Spain). Results from the core AÑ2 suggest that the concentration-dependent magnetic parameters mainly reflect variations in the content of detrital magnetite, sourced in the catchment rocks and soils of the basin, via changes in the dynamics of alluvial fans due to temperature changes in the northern hemisphere during the Late Pleistocene. The correspondence between the magnetic proxies and the temperature variations in the North Atlantic region (NGRIP curve) indicates that higher (lower) concentrations and finer (coarser) magnetite grains coincide with warm (cold) periods. We propose that during cold periods, a sparser vegetation cover favored the incoming of higher energy runoff bearing coarser sediments to the basin that are relatively impoverished in magnetite. In contrast, during warm periods, the wider distribution of the vegetation cover associated with the lower runoff energy lead to finer, magnetite-richer sediment input to the basin. Maghemite, presumably of pedogenic origin, appears to be present also in the studied alluvial sediments. Further studies are necessary to unravel its palaeoclimatic significance.

KEYWORDS | **Magnetite. Environmental magnetism. Añavieja Basin. Alluvial sequence. Vegetation cover. Temperature. NGRIP curve.**

INTRODUCTION

The Iberian Peninsula is located in the western Mediterranean region, potentially one of the most sensitive areas to future climate changes (Giorgi, 2006; Giorgi and Lionello, 2008; Lionello, 2012). Due to its position under the influence of Atlantic and Mediterranean climates, the Iberian Peninsula has provided a wealth of data on the variability and interaction of both climate systems (Cacho *et al*., 2001; Moreno *et al*., 2005; Hurrel and Deser, 2009). During the last glacial cycle, Dansgaard-Oeschger oscillations have been identified in marine sediments surrounding Iberia, with Heinrich events (HE) being reported as cold and dry periods (*e.g*. Cacho *et al*., 1999, 2001; Moreno *et al*., 2002; Sánchez-Goñi *et al*., 2002; Fletcher and Sanchez-Goñi, 2008). Data from continental sequences in the Iberian Peninsula, related to temperature and water availability for late glacial and last deglaciation period allow the identification of these signals on land.

Lacustrine sediments (Valero-Garcés and Moreno, 2011) and speleothems (Domínguez-Villar *et al*., 2008) are the continental records from which most data based on different proxies for climate variability (*e.g*. pollen, mineralogy, geochemistry) have been produced in the Iberian Peninsula. Overall, these records corroborate previous observations in marine sediments. In general, assessing a link between climate variability in the Iberian Peninsula and rapid climatic changes in the North Atlantic region has proven difficult, specially for the last glacial transition, because precisely dated palaeoclimatic records are restricted to few records such as those from Estanya Lake (Morellón *et al*., 2009), Banyoles Lake (Pérez-Obiol and Julià, 1994; Valero-Garcés *et al*., 1998), Pla d'Estany (Burjachs, 1994), Enol Lake (Moreno *et al*., 2010b), Portalet peat bog (González-Sampériz *et al*., 2006), Padul peat bog (Ortiz *et al*., 2010), Pindal Cave (Moreno *et al*., 2010a) and Abric Romaní rock-shelter (Burjachs *et al*., 2012).

Although less studied, alluvial systems have also proven to be excellent indicators of palaeoenvironmental variations, particularly due to their fast response to climate changes (Eybergen and Imeson, 1989; Waters and Haynes, 2001; Viles and Goudie, 2003; Faust *et al*., 2004; Benito *et al*., 2008; Dorn, 2009; Schulte *et al*., 2015). The main problem related to alluvial systems is that it is difficult to establish high-resolution chronologies and obtain reliable proxies for environmental change. Sedimentation is supposed to be often discontinuous but, in many cases, periods of low or non-sedimentation are commonly registered by soil formation. In the last two decades, several studies based on alluvial systems and other continental sediments have contributed to understand climate variability in the Iberian Peninsula and its relation to other nearby areas (Fang *et al*., 1999; Schulte, 2002; Harvey *et al*., 2003; Faust *et al*., 2004; Zielhofer and Faust, 2008; Thorndycraft and Benito, 2006; Sancho *et al*., 2008; Schulte *et al*., 2008; Uribelarrea and Benito, 2008; Bastida *et al*., 2013). In this context, magnetic methods provide valuable complementary data which, in combination with sedimentological interpretations, have been demonstrated to provide reliable indicators of palaeoenvironmental changes in alluvial sediments (White and Walden, 1997; Pope and Millington, 2000; Pope *et al*., 2003; Pope *et al*., 2008; Liu *et al*., 2012; Gómez-Paccard *et al*., 2013).

Here we applied this combined approach of sedimentological and magnetic signatures, to the study of a Late Pleistocene alluvial sequence recovered in a drill hole from the Añavieja Basin in the Iberian Range (NE Spain). This sequence provides a better understanding of the climate variability experienced by the Iberian Peninsula during the last glacial transition in mountainous regions, complementing other palaeoclimatic records derived from lake and peat bog sediments (González-Sampériz *et al*., 2006; Morellón *et al*., 2009; Jambrina *et al*., 2011) and speleothems (Moreno *et al*., 2010a). Our study highlights the need for considering alluvial sediments as prime targets in palaeoclimate studies and provides conclusive evidence of the usefulness of integrating environmental magnetic proxies in palaeoenvironmental studies.

GEOLOGICAL SETTING

The Añavieja Basin (1000m.a.s.l., metres above sea level) is located in the NW sector of the Iberian Range (Spain), at the headwaters of the Añamaza River. The present-day climate in the area is described as Cfb in the Köppen classification (Köppen, 1936) and corresponds to a temperate climate without a dry season characterized by cool summers and winters (maximum temperature range in 2014 was between -5ºC and 34ºC).

Alluvial fans spreading from the margins of the Añavieja Basin occupied most of the central part of the basin during the Late Pleistocene, and connected downstream with tufa-dominated fluvial areas (Luzón *et al*., 2011; Arenas *et al*., 2014). The sedimentary system had a catchment area of about 140km^2, with water supplies including superficial and groundwater discharges. During the Holocene, a shallow lake (Añavieja Lake) developed in the distal alluvial zone. The lake had a mean surface area of 5km^2 and was artificially drained around 1866.

In the study area, the Pleistocene deposits overlie Mesozoic (Middle Jurassic, Early Cretaceous) and Cenozoic (Neogene) units (Fig. 1). Middle Jurassic marine carbonates (Chelva Formation), fluvial sandstones

Geologica Acta, 14(2), 139-154 (2016)
DOI: 10.1344/GeologicaActa2016.14.2.4

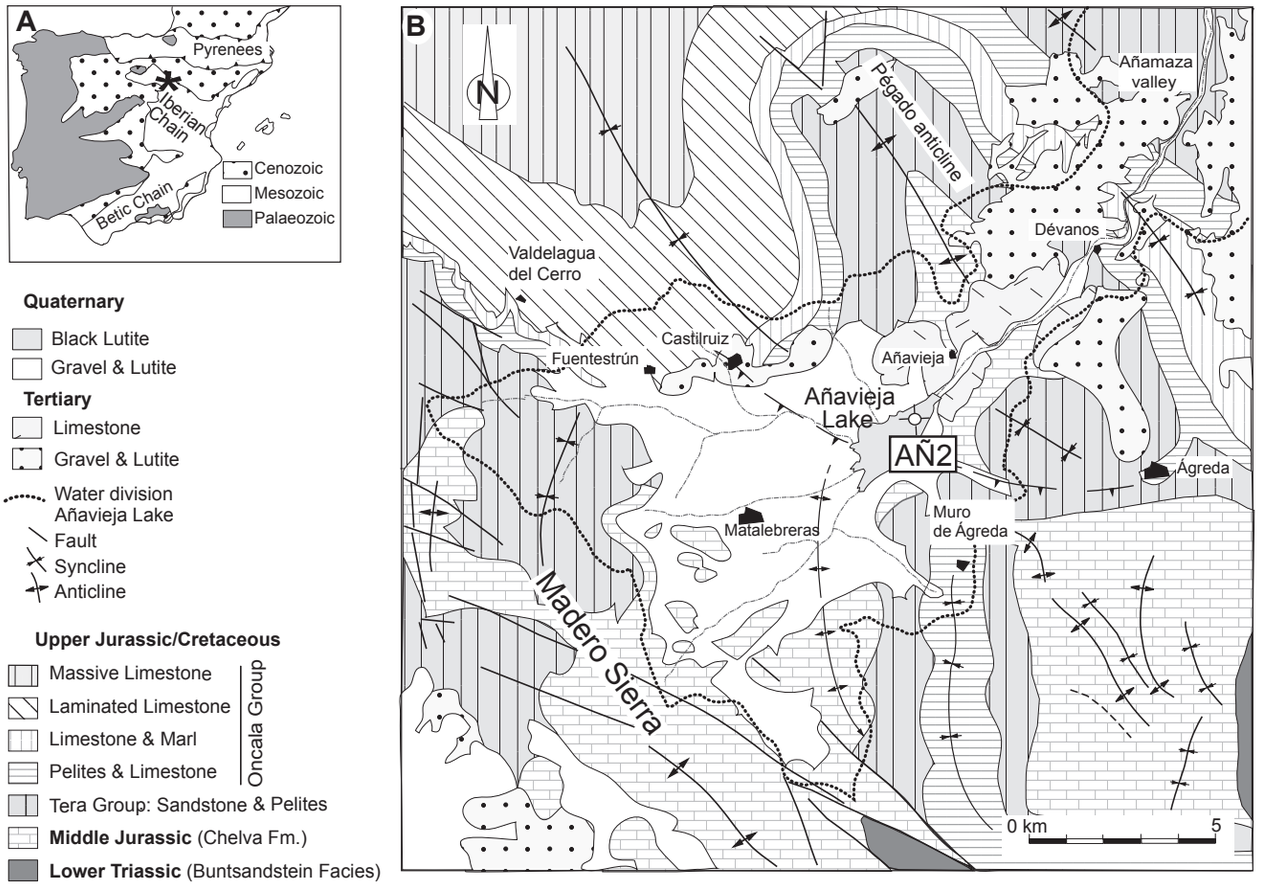

FIGURE 1. A) Location of the study area in the Iberian Peninsula marked with a star. B) Detailed geological map of the study area.

and siltstones of Jurassic-Cretaceous age (Tera Group), and Lower Cretaceous lacustrine limestones (Oncala Group) integrate the Mesozoic succession. Continental conglomerates, siltstones and limestones compose the Cenozoic succession, which lies subhorizontally and unconformably over the Mesozoic rocks. Tectonic structures (folds and faults) affecting the Mesozoic succession follow a general NW-SE trend. Previous palaeomagnetic studies in nearby areas have shown that fine-grained magnetite is the main ferromagnetic mineral in the Jurassic marine limestones (Juárez *et al.*, 1998), that constitute around 50% of the catchment area of the Añavieja Basin (Fig. 1). Magnetite and hematite are the most common ferromagnetic minerals in the Tera and Oncala groups, that account for about 30% and 10% of the catchment area, respectively (Villalaín *et al.*, 2003).

MATERIALS AND METHODS

The core AÑ2 (30TWM835536) (41°52'7.69"N, 1°59'32.91"W) was drilled in March 2008 near the eastern margin of the Añavieja Basin (Fig. 1) using a rotatory RL-48-L core drill. The core was transported to the Sedimentology Laboratory of the Zaragoza University where it was kept in humid conditions (more than 95% humidity). The subsequent study of the core was carried out following the protocol recommended by the Limnological Research Centre (Minneapolis, USA), especially for the Initial Core Description (Schnurrenberger *et al.*, 2003). In the laboratory, the core was described, photographed, measured, sampled and split. Description of the core included lithology, colour, grain size, sedimentary structures and biological content. A facies analysis was carried out in order to interpret sedimentary processes.

The chronology of the core section is based on radiocarbon dating of six bulk organic matter samples (Table 1), as terrestrial organic remains were not found. Three of these samples were analysed in a previous work (Luzón *et al.*, 2011), and chronological data from 3 new samples (AÑ2-71, AÑ2-77 and AÑ2-108) a included here. These samples were prepared and analyzed in the

Beta Analytic Radiocarbon Dating Laboratory of Florida (USA). ^{14}C ages were calibrated using the radiocarbon calibration program INTCAL09 database (Reimer *et al.*, 2009). In order to improve the chronology of the studied succession we also applied an alternative dating method, the Optically Stimulated Luminiscence (OSL), but results have not been satisfactory.

The carbonate content of 193 selected samples from the Late Pleistocene deposits, (from the lower 19.3m of the AÑ2 core, at 10cm intervals) was analyzed with a Geoservices calcimeter at the University of Zaragoza that calculated the total percentage of carbonate and the calcite/dolomite ratio. Grain size of the same samples was determined by light scattering in the Sedimentology Laboratory of the Barcelona University using a Coulter LS 230 device.

Chemical and morphological analyses of some samples were performed in a Carl Zeiss MERLIN Field Emission Scanning Electron Microscope (FESEM) using secondary electron imaging.

Sampling for environmental magnetic measurements was done with a 5cm resolution (386 samples) using a water-refrigerated portable electric drill machine. Bulk environmental magnetic properties of the standard samples included: i) the low field magnetic susceptibility measured with a KLY-3S susceptometer (AGICO, Inc.); ii) Anhysteretic Remanent Magnetization (ARM) applied with a 2G demagnetization unit (Model 615) in a Direct Current (DC) bias field of 50μT parallel to the Alternating Field (AF) of 100mT peak, ARM is further expressed as the χ_{ARM} defined as ARM/DC field; iii) an Isothermal Remanent Magnetization (IRM) applied at 1.8T (regarded as the saturation IRM, SIRM564r) with a M2T-1 Pulse Magnetizer. All bulk magnetic properties were normalized by the weight of the samples.

Samples representative of the different bulk environmental magnetic properties were analyzed to establish their magnetic mineralogy. A Magnetic Measurements Variable Field Translation Balance (MMVFTB, Petersen Instruments) was used to measure IRM acquisition curves, back field curves, and hysteresis loops (applied field up to 1T). Thermomagnetic curves were performed with the same instrument by measuring variations of the induced magnetization between room temperature and 700ºC in an applied field of 38mT and an argon atmosphere. In addition, variations of the magnetic susceptibility from room temperature to 700ºC (with a flow of argon) were measured using a KLY-3S-CS3 (AGICO Inc.) susceptibility bridge with a field intensity of 0.38mT and 875Hz of operating frequency. The magnetic susceptibility was measured at two frequencies of 976 and 15616Hz using a MFK (AGICO Inc.) susceptibility bridge. The corresponding k values are referred to k_{LF}

TABLE 1. AMS radiocarbon dates from samples taken in AÑ2 core from the Añavieja Basin. New data are indicated with an asterisk

Depth (m)	Sample code	Lab. Number	$\delta^{13}C$ (‰)	^{14}C date yr. BP	(2s) 95% probability cal. BP range	Cal. yr. BP	Material
0.90	AÑ2-9	UZ-5679/ETH-37058	–24.7	695±30	680-576	636	Bulk sediment
2.5	AÑ2-25	UZ-5680/ETH-37059	–23.7	8200±40	9365-9035	9165	Bulk sediment
7.1	AÑ2-71*	Beta-291591	–26.6	7360±50	8290-8260 and 8210-8020	8170	Bulk sediment
7.7	AÑ2-77*	Beta-289914	–26.9	6360±40	7410-7350 and 7340-7240	7270	Bulk sediment
10.8	AÑ2-108*	Beta-289915	–26.2	11190±50	13190-12980	13100	Bulk sediment
22.2	AÑ2-222	UZ-5681/ETH-37404	–21.9	16170±70	19524-19053	19287	Bulk sediment

Geologica Acta, 14(2), 139-154 (2016)
DOI: 10.1344/GeologicaActa2016.14.2.4

and k_{HF}, respectively. The parameter k_{fd}, defined as $k_{LF} - k_{HF}$, was used to infer the relative concentration of Super Paramagnetic (SP) grains near the SP-Single Domain (SD) boundary (Worm, 1998; Liu *et al.*, 2012).

Once the magnetic mineralogy was identified, we used bivariate plots to study the significance of bulk magnetic properties. Special attention was paid to parameters potentially indicative of magnetic mineralogy (SIRM/χ), concentration (χ, ARM, SIRM), and grain size (SIRM/χ_{ARM}) (Thompson and Oldfield, 1986; Verosub and Roberts, 1995; Peters and Dekkers, 2003; Liu *et al.*, 2012).

Magnetic susceptibility data were measured at the Magnetic Laboratory of the Physical Measurements Service of the University of Zaragoza (Spain), and at the Institute of Geology and Geophysics of the Chinese Academy of Science in Beijing (China). Bulk environmental magnetic properties, IRM acquisition curves, back-field curves, hysteresis loops and thermomagnetic curves were analyzed at the Palaeomagnetic Laboratory of the University of Burgos (Spain).

RESULTS

Chronology

Accelerator mass spectrometry (AMS) ^{14}C data indicate that the uppermost 3m of the core are Holocene in age (Fig. 2) and the underlying sediments are Late Pleistocene. It is worth mentioning that two radiocarbon samples, at 7.1 and 7.7m-depth, provided anomalous results as both yield ages younger than that obtained at 2.5m (Table 1, AÑ2-25). They have been rejected considering that:

i) the organic content was considerably higher in AÑ2-25, this sample is considered to be the most reliable dating;

ii) the gravel deposits at ~6m correspond to a cold episode recorded in other areas (Younger Dryas; González-Sampériz *et al.*, 2006; Luzón *et al.*, 2007; Sancho *et al.*, 2008);

iii) the rejected ages are similar to the one at ~2.5m, when more humid conditions favoured a wide vegetation cover which produced penetration of tree roots at greater depths or infiltration of carbonate towards the lower parts of the soil profile (Luzón *et al.*, 2012). A similar scenario has been described by Andrés *et al.* (2002). In this sense, organic matter used for dating at 2.5m-depth would be *in situ*;

iv) sedimentation rates are consistent after rejecting outlying samples. In addition, the two lowermost samples (AÑ2-108 and AÑ2-222) indicate a Late Pleistocene age (<20,000 cal yr BP) for the rest of the core.

Sedimentology

AÑ2 core consists of a 25.3m thick sequence of red and brown mudstones with interbedded sand and gravel beds up to 1m thick (Fig. 2). Based on lithology, colour and grain size, four main lithofacies have been differentiated: massive brown gravels (Gm), brown and rare red sands and silts (S), brown and ochre mudstone (Mb) and grey and black mudstone (Mg). Their main features and interpretation are summarized in Table 2. As neither the geometry, nor large-scale sedimentary structures could be observed in the core, interpretation of sedimentary processes has been mainly based on macroscopic characteristics, carbonate content and grain size analysis. Grain size distribution (Visher, 1969) indicates that the studied materials were transported as suspended load in water runoff and mainly deposited by settling. These facies are grouped in three main facies associations, namely A to C (Fig. 3) that represent distinct sedimentary processes and subenvironments. Facies association A is fining upwards, and is composed of brown gravels (Gm) that grade upwards into brown to red silty sands and sands (S) and, finally, into brown mudstone (Mb). Gravels are not always present. Mudstone display horizontal lamination and bioturbation. Facies association B is composed of brown bioturbated mudstone (Mb) with manganese stains in the lower part and white carbonate nodules towards the top. Facies association C consist of ochre and grey mudstone with carbonate nodules (Mb), that pass into laminated, grey and black mudstone towards the top (Mg). Sedimentary facies are delineated by quantitative grain sized data, so that mudstone are typically enriched in clay-sized (<1μm) particles (Fig. 2). Carbonate content is higher in the lower and upper part of the Pleistocene series.

The Late Pleistocene interval of the sediment core includes associations A and B that can be interpreted as deposited in an alluvial plain setting (Hogg, 1982; Huerta and Armenteros, 2005, Luzón, 2005; Pla-Pueyo *et al.*, 2009). Gravels mainly appear in the upper part of the Pleistocene series. Coarse terrigenous fraction (gravel and sand) in facies association A is interpreted as related to sheet floods generated during periods of higher water and sediment discharge with mudstone settled out during less energetic runoffs. Facies association B features imply low sedimentary rates that favored vegetation growth and bioturbation. Manganese stains are related to hydromorphic conditions whereas carbonate nodules

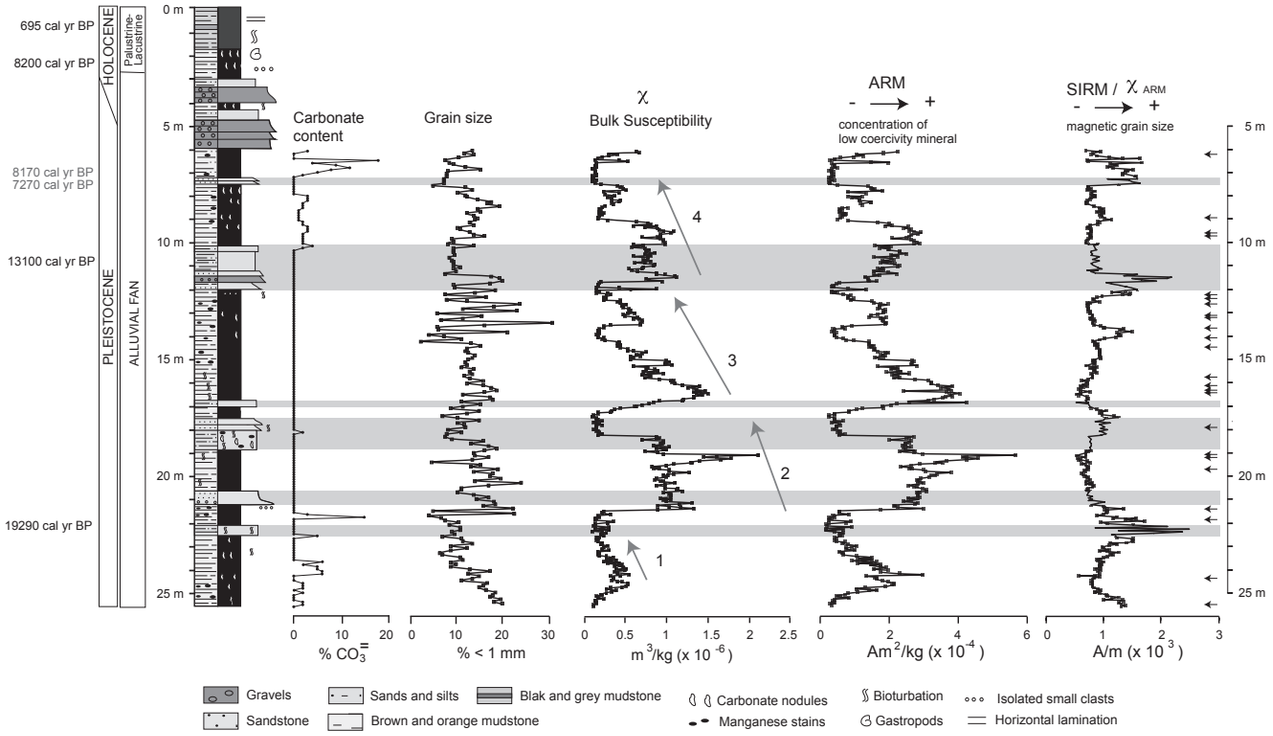

FIGURE 2. Sedimentological profile, carbonate content, grain size (<1μm) and magnetic parameters (mass-specific magnetic susceptibility, χ; anisotropy of the Anhysteretic Remanence Magnetization (ARM); and the SIRM/χ_{ARM} ratio) of the studied core. All magnetic parameters are normalized by mass. Grey areas mark intervals with coarser grain sizes: gravels, sands and silts. Sample depth to specify magnetic mineralogy are marked on the right with arrows. See text for more details.

indicate carbonate availability and general arid-semiarid conditions during soil formation (Alonso-Zarza, 2003). Facies association C is only present in the upper part of the section, of Holocene age. It represents sedimentation in a shallow lake (Luzón *et al.*, 2011), thereby suggesting a noticeable environmental change with respect to the underlying deposits. This change agrees with increasing lake levels recorded in other Spanish areas related with a relatively warm period at the beginning of the Holocene (Peñalba *et al.*, 1997; Giralt *et al.*, 1999; Valero Garcés *et al.*, 2001; Luzón *et al.*, 2007; Morellón *et al.*, 2009), in agreement with the proposed age model. AMS ^{14}C dating suggests high sedimentary rates for the Late Pleistocene alluvial facies.

Environmental magnetic data

The studied samples can be grouped into two main types. IRM acquisition curves and back-field data indicate that type 1 samples (characterized by high χ and ARM values) are dominated by a low coercivity mineral, which is identified as magnetite on the basis of the main decay observed below 580°C both in the magnetic susceptibility and the induced magnetization curves (Fig. 4A). Thermomagnetic data indicate that the main magnetic mineral in type 2 samples (characterized by low χ and ARM values) is also (low-Ti) magnetite, as indicated by reduced Curie temperature of <580-550°C inferred from the χ-T and induced magnetization curves (Fig. 4B). In this sample type, however, a final decay observed in the thermomagnetic runs above ~580°C indicates that contributions from hematite are also significant (Fig. 4B). The subtle inflection in the magnetic susceptibility heating curve between 350 and 450ºC and the lower magnetic susceptibility signal in the cooling curve indicate the presence of some maghemite in both types of samples (Liu *et al.*, 2005). In type 2 samples the presence of maghemite is further evidenced by its transformation to hematite (as seen in the temperature of the final decay of the magnetic susceptibility, Fig. 4B). Overall, thermomagnetic experiments indicate the presence of (low-Ti) magnetite and smaller amounts of maghemite in the studied alluvial sediments.

The good correlation observed in the bivariate plots relating χ, ARM and SIRM (Fig. 5A, B) indicates that variations in these parameters are mainly dominated by changes in the concentration of the magnetite minerals present, mainly magnetite. SIRM/χ_{ARM}

values range between 0.5 and 2.2kA/m, suggesting the predominance of fine-grained magnetite particles within the SD and Pseudo-SD (PSD) grain size range (<1μm) (see Peters and Dekkers, 2003). The k_{fd} values indicate also the presence of smaller SP ferrimagnetic grains (~20-25nm). This mixture is consistent with the hysteresis data, which demonstrate that the studied samples fall in the PSD grain size region of the Day plot along the trend that represents assemblages of SP and SD particles (Dunlop, 2002). Grain size variations as marked by SIRM/χ_{ARM} values, are often linked to changes in sedimentary facies. Thus, as a general aspect, sand beds contain in general coarser magnetic grain sizes, whereas mudstone contain finer magnetic grains (Fig. 2). Yet, it appears that magnetic data delineate intervals with coarser magnetic grains that do not correspond to sandstone or gravel layers and that are not equally well identified in bulk sediment grain size parameters (Fig. 2). On the other hand, magnetite grain sizes covary with changes in the concentration of magnetite (Fig. 2), as is evident also in the biplot relating SIRM/χ_{ARM} and ARM (Fig. 5C). Thus, higher and lower magnetite concentrations are characterized by finer and coarser magnetite grain sizes, respectively. Moreover, k_{fd} values show a positive correlation with ARM (Fig. 5D), which indicates that the concentration of SP grains covaries with that of the bulk magnetite content.

The coupled stratigraphic variations of χ, ARM and SIRM (Fig. 2) demonstrate that the concentration of magnetite displays a saw-tooth pattern that is unrelated to variations in the relative concentration of pedogenetic manganese and carbonate nodules (Fig. 2). Such a pattern is characterized by four ~5m-thick cycles that begin with a sharp increase in the concentration of magnetite and continue with a more gradual decrease that is specially evident in cycles 2, 3 and 4 (meters 22.5-17.5, 16.5-12 and 11.5-7). This saw-tooth pattern is marked by an overall upwards decrease in the maximum concentration of magnetite up from the second cycle (Fig. 2). The lowest concentrations of magnetite are often associated with sedimentary facies association A that includes coarse-grained sediments such as sands and gravels (*i.e.* at around 18, 12 and 7.2m depth).

TABLE 2. Sedimentary facies registered in the AÑ2 core in the Añavieja Basin

Facies	Description	Interpretation
Gm: Brown gravels	Massive and grain-supported gravels with sandy or muddy matrix and rounded to subrounded siliceous and carbonate cm-scale clasts in 20 to 55 cm-thick levels.	Tractive flows and development of gravel sheets. High-energy discharges in the alluvial plane.
S: Brown and rare red sands and silts	Massive fine to very coarse sands and silts (cm-dm thick levels) with horizontal lamination and scarce bioturbation. Some manganese stains.	Sheet floods in the alluvial plain. Pedogenic processes after deposition.
Mb: Brown and ochre mudstones	Massive and bioturbated lutites and sandy mudstones (cm-m thick levels). Common manganese stains and white carbonate nodules. Dispersed clasts.	Fine terrigenous settling and development of pedogenic processes in the alluvial plains.
Mg: Grey and black mudstones	Laminated mudstones in 10 to 20 cm-thick levels with interbedded yellow laminae. Gastropods and macrophyte remains.	Mudstone settling in a perennial-semiperennial fresh water body. Anoxic conditions allowed organic matter preservation.

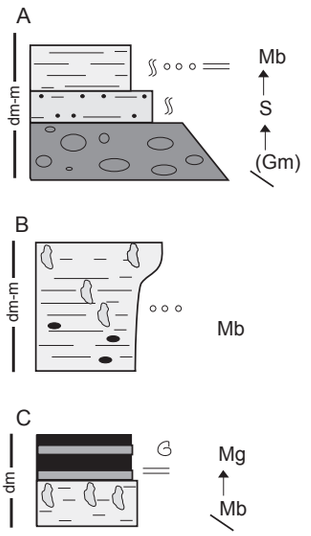

FIGURE 3. Facies associations defined in the AÑ2 core. Lithofacies acronyms correspond to those in Table 2. Gravels, sands and silts in facies association A represent sheet floods generated during high water and sediment discharges; mudstones settled out during less energetic floods. Facies association B is related to favorable conditions for vegetation growth on previously deposited materials in the distal alluvial plain. Association C represents sedimentation in a shallow fresh water lake. For legend, see Figure 2 and Table 2.

DISCUSSION

Sedimentary system evolution

During the Late Pleistocene, small alluvial fans spread from surrounding source areas towards the centre of the Añavieja Basin. Proximal alluvial sectors were less than 5km long and distal sectors covered the main part of the basin (Fig. 6). Taking into account the geographical location of the AÑ2 core, its main feeding system would be constrained to the Muro de Ágreda syncline, including Middle Jurassic to Cretaceous rocks (Fig. 1). The general alluvial progradation in the Añavieja Basin during the latest Pleistocene could be favored by increasing aridity and coldness, which is

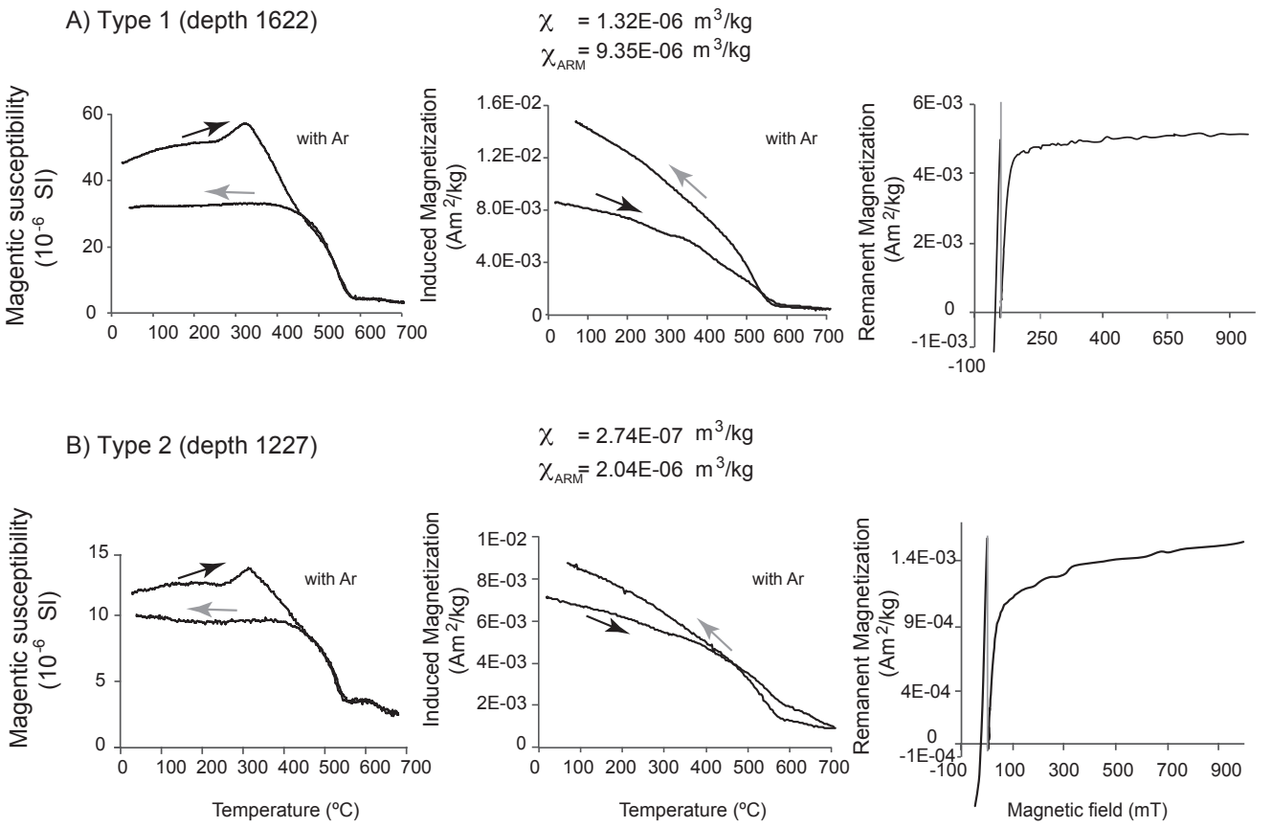

FIGURE 4. Rock magnetic analyses A) type 1 and B) type 2 of samples described in the text. From left to right: k-T curves (temperature dependent magnetic susceptibility), temperature dependent induced magnetization, and the isothermal remanent magnetization acquisition curve (right) with the back field (left).

consistent with the climatic conditions reconstructed from sediments of this age in the Ebro Basin and other areas of the Iberian Range (Andrés *et al.*, 2002; Luzón *et al.*, 2007; Bastida *et al.*, 2013).

Sedimentary facies changes in the AÑ2 core are interpreted as related to changes in runoff energy, the intensity of the discharge being conditioned by vegetation cover and hydrology. Climate controls sediment supply within upland drainage systems through vegetation expansion/retraction (Macklin and Fuller, 2002), which has implications for discharge to sediment load ratio (Langbein and Schumm, 1958; Pope and Wilkinson, 2006). During drier stages the vegetation cover would be reduced resulting in increased flooding and sediment transport (Rohdenburg, 1989; Giessner, 1990; White *et al.*, 1996; Faust *et al.*, 2004; Fenech, 2007; Sancho *et al.*, 2008; Vásquez-Méndez *et al.*, 2010). Thus, we interpret that coarser sediments would reach the location of the core during periods of stronger water discharges, and less vegetated source areas. Mudstone would be associated with denser vegetation cover stages with soil development and catchment areas protected from erosive processes (Fig. 7). Mudstone in the distal alluvial plain show evidences of soil development during these stages. Carbonate nodules indicate alkaline conditions and an arid-semiarid setting (Alonso-Zarza, 2003) that also favored manganese oxides precipitation (Fig. 2B). This interpretation is in line with previous works in other areas where landscapes with decreased frequency flooding under more humid conditions are interpreted as the result of denser vegetation cover, soil formation and low surface runoff (Frenzel *et al.*, 1992; Pope and Wilkinson, 2005; Fletcher and Zielhofer, 2013 and references therein).

Finally, the considerably moister conditions reached at the beginning of the Holocene would have caused a sharp retrogradation of the alluvial fans and the expansion of the Añavieja Lake (Luzón *et al.*, 2007; Luzón *et al.*, 2011), Figure 7. This scenario agrees with the increasing of the vegetation cover in the Añavieja Basin (Luzón *et al.*, 2012) and the overall wetter climate that prevailed in the Iberian Peninsula at the beginning of the Holocene (Valero-Garcés *et al.*, 1998; Muñoz-

Geologica Acta, 14(2), 139-154 (2016)
DOI: 10.1344/GeologicaActa2016.14.2.4

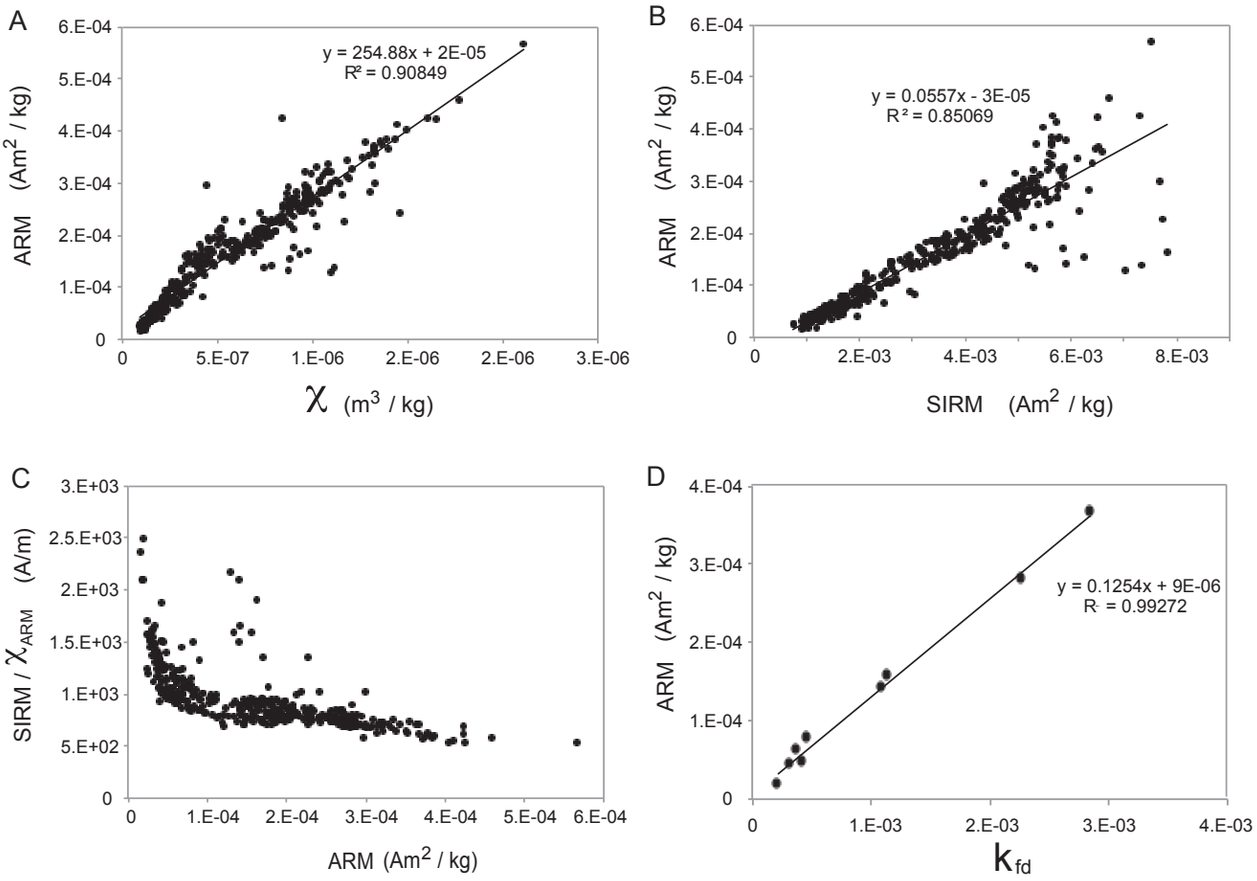

FIGURE 5. Biplots of magnetic parameters, A) ARM against χ, B) ARM against SIRM, C) SIRM/χ_{ARM} against ARM and D) ARM against k_{fd}.

Sobrino *et al.*, 2004; Morellón *et al.*, 2009; Pérez-Obiol *et al.*, 2011). This change from alluvial to lacustrine sedimentation associated to the Pleistocene-Holocene transition has also been described in other zones of the Iberian Range (*e.g.* Luzón *et al.*, 2007).

Origin and significance of magnetic minerals

The magnetic assemblage consists mainly of fine-grained magnetite and maghemite. Magnetite in the studied sediments might have three different origins. First, it might be a detrital mineral eroded from the SP/SD magnetite-bearing Jurassic and Cretaceous sedimentary rocks of the catchment area (Juárez *et al.*, 1998; Villalaín *et al.*, 2003). Second, magnetite might have formed by enhanced pedogenic processes in soils of the Añavieja catchment during warmer periods. Pedogenic magnetite is typically fine grained (Evans and Heller, 2003; Liu *et al.*, 2012), hence it might have contributed to increase the budget of original fine-grained magnetite particles in the catchment rocks that was then ready for terrigenous transport down the alluvial system. And third, fine-grained magnetite particles could have formed *in-situ* via pedogenesis. We discard this last option since concentration-dependent parameters show no clear link with intervals where manganese and carbonate nodules show highest concentrations. Therefore, we interpret that magnetite in the studied sediments is detrital and sourced from the Jurassic and Cretaceous sedimentary rocks and soils of the catchment of the Añavieja Basin. With regards to maghemite, it is a magnetic mineral that forms typically during pedogenesis as nanosized particles (*e.g.* SP) in continental environments (*e.g.* Liu *et al.*, 2012). A pedogenic origin for maghemite in the alluvial sediments of the Añavieja Basin is therefore the most likely possibility. However, it might be a detrital mineral eroded from the soils of the Añavieja catchment. Further analyses (*e.g.* high-resolution k_{fd} measurements) and its comparison with sedimentological data are needed in order to constrain the origin and palaeoclimatic significance of maghemite.

In summary, the variations in the content and grain size of magnetite show a broad correspondence with

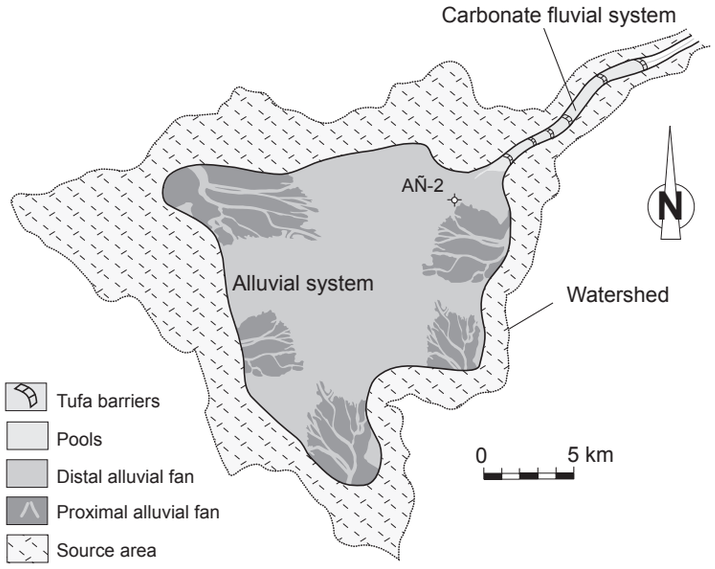

FIGURE 6. Palaeogeographical map for the Añavieja sedimentary basin. AÑ2 refers to the core location.

sedimentary facies (Fig. 2), so that finer sediments are characterized by higher concentrations and larger contents of finer magnetite grains and coarser sediments by higher concentrations of coarser-grained magnetite and lower concentrations of this mineral. Overall, these data are consistent with a detrital origin of magnetite in the studied sediments from the AÑ2 core, either from the source rock area and/or soils developed on top of the source rock area. Concentration-dependent magnetic parameters display cyclic variations regardless of the relative abundance of manganese stains or carbonate nodules (Fig. 2), which excludes *in-situ* pedogenic processes (within the studied alluvial sediments) as the putative mechanism leading to variations in the concentration of magnetite.

Palaeoclimatic implications

Radiocarbon dates do not enable us to obtain a precise chronological model for the AÑ2 core. Nevertheless, they indicate that the analyzed sediments accumulated after ~20kyr BP and before the beginning of the Holocene (~11kyr BP) (Fig. 2). Inspection of magnetic data reveals a resemblance of the magnetite content changes (as marked by χ, ARM and SIRM) with the $\delta^{18}O$ curve from the NGRIP ice-core (Rasmussen *et al.*, 2008) between 12.1 and 15.4kyr (Fig. 8). Thus, the saw-tooth pattern observed in the χ record between meters 9 and 21 clearly resembles that of the period that spans the Bølling-Allerød interstadial and culminates with the Younger Dryas cooling. SIRM/χ_{ARM} also shows some correspondence with the $\delta^{18}O$ NGRIP ice-core record, but due to its more gradual pattern of variability such correspondence is not as clear as that of the concentration-dependent parameters. Based on this peak-to-peak correspondence, we have developed an age model for the studied sediments of AÑ2 core by tuning the main features of the χ record to the ice $\delta^{18}O$ curve from the NGRIP (Fig. 8). Linear interpolation done with Analyseries 2.0 (Paillard *et al.*, 1996) between six tie points has been used to calculate the age of the studied interval. This age model suggests that the studied alluvial sediments accumulated between 12.1 and 15.4kyr BP have an average accumulation rate of around 5.5mm yr^{-1} (Fig. 8).

This proposed correlation implies variations in the concentration of detrital magnetite in the studied sediments, in response to temperature changes driven by abrupt climate changes recorded in the North Atlantic region. Changes in magnetic grain size appear to respond to temperature changes in a more gradual fashion (Fig. 2). Two main issues need to be kept in mind in order to interpret the environmental magnetic properties of core AÑ2, the detrital origin inferred for magnetite and maghemite and the sedimentary model of the Añavieja Basin, which links climate to sedimentary grain size via changes in vegetation cover and runoff energy. We propose that coupled changes in the concentration and grain size of ferromagnetic *sensu lato* (s.l.) minerals can be explained in terms of

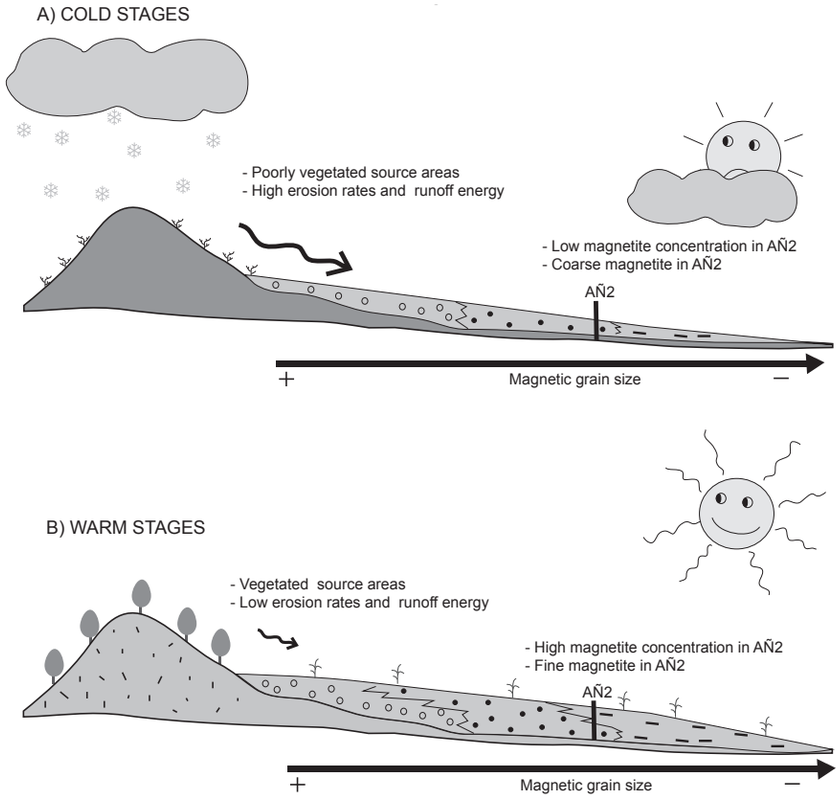

FIGURE 7. Conceptual environmental model deduced from the magnetic record in Añavieja core, with two climate scenarios in the Añavieja Basin. It links climate with hydrology, lithology, magnetite grain size and magnetite concentration in the alluvial sediments. AÑ2 core location has been selected as reference zone. A) Cold stages in the North Atlantic area corresponded to cold stages in the Iberian Range. Vegetation cover density decreased and runoff energy increased carrying coarser detrital sediments (including coarse-grained magnetite) to the distal alluvial setting (AÑ2 core area). As in the source areas of the basin fine magnetite predominates, the major concentrations of such mineral would be registered in more distal areas. B) Warm stages in the North Atlantic area corresponded to warm stages in the Iberian Range. Vegetation cover increased and runoff energy decreased. This situation favored a general retrogradation of the alluvial system. Fine-grained, magnetite-rich sediments will be deposited at the AÑ2 core site whereas coarser sediments will be deposited upstream this zone.

the effect of hydrodynamic sorting on the terrigenous fraction of the Añavieja alluvial system, as follows. Cold periods are likely to reduce the vegetation cover, and hence are expected to increase the runoff energy (Fig. 7). We infer that, at the location of the AÑ2 core, sedimentation will then experience a significant coarsening, with finer, magnetite-enriched sediments being transported towards areas located downstream of the AÑ2 core site. During warmer phases, the expansion of vegetation cover could decrease the runoff energy. In consequence, finer grained, magnetite-rich sediments will be deposited at the studied site with coarser sediments being deposited upstream of this zone. The more gradual correlation observed between magnetite grain size and the $\delta^{18}O$ NGRIP ice-core record as compared to magnetite concentration might be due to other mechanisms affecting vegetation cover, in addition to temperature, such as for example changes in the type of precipitation. If carbonate concentration is also considered and compared with the NGRIP curve, it emerges that carbonate precipitation was also related to climate, being favored during the colder and arid stages (as seen in Rowe and Maher, 2000).

CONCLUSIONS

The magnetic analyses carried out in the Late Pleistocene alluvial fan sequence at Añavieja Basin allow distinguishing variations in the content of fine-grained detrital magnetite along the core. The radiocarbon-based age model proposed for the AÑ2 core is far from being robust, as it occurs in many other Quaternary continental records. It suffices, however, to propose an age for the record from 20 to 11kyr BP. With this caveat in mind, we observe a correspondence between the concentration of strongly magnetic minerals and the $\delta^{18}O$ curve of the NGRIP ice-core between 12.1 and 15.4kyr BP. We interpret this match as indicating a quick

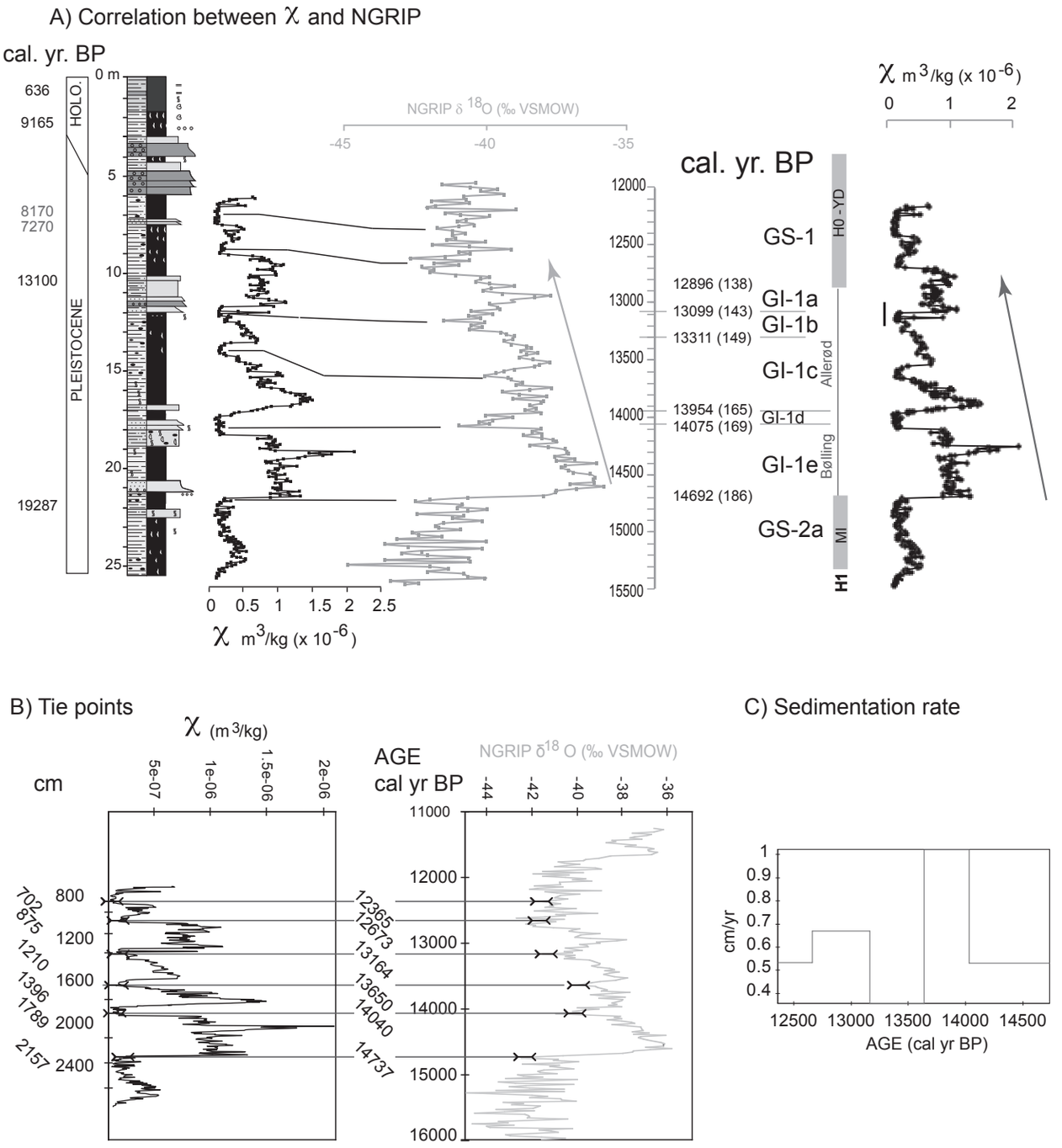

FIGURE 8. A) Proposed correlation between magnetic susceptibility data from AÑ2 core (proxy for magnetite concentration) and $\delta^{18}O$ data from NGRIP ice core to convert depth into time scale. B) Tie points used for the correlation with Analyseries 2.0. C) Sedimentation rate. Time-stratigraphic divisions follow Lowe *et al.*, 2008 (INTIMATE working group).

response of the Añavieja alluvial system to temperature variations in the North Atlantic, via changes in runoff energy conditioned by vegetation cover and hydrology. Thus, higher concentrations and finer magnetic grains coincide with warm periods during which vegetation spreads through the catchment, decreasing runoff energy. Higher concentrations of coarser magnetite grains were reported during colder periods characterized by a decreased vegetation cover. Maghemite appears to be present also in alluvial sediments from the Añavieja

Geologica Acta, 14(2), 139-154 (2016)
DOI: 10.1344/GeologicaActa2016.14.2.4

Basin, but unraveling its origin (pedogenic or detrital) and palaeoclimatic significance demands further studies.

ACKNOWLEDGMENTS

BOU acknowledges a JAEDoc contract in the CSIC co-financed by the ESF. This study has been supported by research projects CGL2009-09165/BTE and CGL2009-08969, funded by the Ministerio de Ciencia e Innovación from Spain and FEDER UZ 2008-CIE-12. The Groups "Análisis de cuencas sedimentarias continentales" (E-28), "Geotransfer" and "Geomorfología y Cambio Global" (E-68) of the Aragón Government Fondo Social Europeo also supported the study. Q. Liu thanks support from the Chinese Academy of Sciences. We are also grateful to Violeta Borruel for her help during palaeomagnetic sampling. Thanks to Dr. Juan José Villalaín, who provided us with access to the Palaeomagnetic Laboratory of the University of Burgos and Dra. Mª José Mayayo for support in the textural study.

REFERENCES

Alonso Zarza, A.M., 2003. Paleoenvironmental significance of palustrine carbonates and calcretes in the geological record. Earth-Science Reviews, 60, 261-298.

Andrés, A., Ries, J., Seeger, M., 2002. Pre-Holocene sediments in the Barranco de las Lenas, Central Ebro Basin, Spain, as indicators for climate-induced fluvial activities. Quaternary International, 93-94, 65-72.

Arenas, C., Vázquez-Urbez, M., Pardo, G., Sancho, C., 2014. Sedimentology and depositional architecture of tufas deposited in stepped fluvial systems of changing slope: lessons from the Quaternary Añamaza valley (Iberian Range, Spain). Sedimentology, 61, 133-171.

Bastida, J., Osácar, M.C., Sancho, C., Muñoz, A., 2013. Environmental changes during the upper Pleistocene-Holocene in mediterranean NE Spain as recorded by the mineralogy and geochemistry of alluvial records. Quaternary International, 302, 3-19.

Benito, G., Thorndycraft, V.R., Rico, M., Sánchez-Moya, Y., Sopena, A., 2008. Palaeoflood and floodplain records from Spain: evidence for long-term climate variability and environmental changes. Geomorphology, 101, 68-77.

Burjachs, F., 1994. The palynology of the upper pleistocene and holocene of the north east Iberian Peninsula: Pla de l'Estany (Catalonia). Historical Biology, 9, 17-33.

Burjachs, F., López-García, J.M., Allué, E., Blain, H.-A., Rivals, F., Bennàsar, M., Expósito, I., 2012. Palaeoecology of Neanderthals during Dansgaarde Oeschger cycles in northeastern Iberia (Abric Romaní): From regional to global scale. Quaternary International, 247, 26-37.

Cacho, I., Grimalt, J.O., Pelejero, C., Canals, M., Sierro, F.J., Flores, J.A., Shackleton, N.J., 1999. Dansgaard-Oeschger and Heinrich event imprints in the Alboran Sea paleotemperatures. Paleoceanography, 14, 698-705.

Cacho, I., Grimalt, J.O., Canals, M., Sbaffi, L., Shackleton, N.J., Schönfeld, J., Zahn, R., 2001. Variability of the Western Mediterranean sea surface temperatures during the last 25,000 years and its connection with the northern hemisphere climatic changes. Paleoceanography, 16, 40-52.

Domínguez-Villar, D., Wang, X., Cheng, H., Martín-Chivelet, J., Edwards R.L., 2008. A high-resolution late Holocene speleothem record from Kaite Cave, northern Spain: $\delta^{18}O$ variability and possible causes. Quaternary International, 187(1), 40-51.

Dorn, R.I., 2009. The Role of Climatic Change in Alluvial Fan Development. In: Parsons, A.J., Abrahams, A.D. (eds.). Geomorphology of Desert Environments. Springer Science+Business Media B.V., 2nd ed., 723-742. DOI 10.1007/978-1-4020-5719-9 24

Dunlop, D., 2002. Theory and application of the Day plot (Mrs/Ms versus Hcr/Hc). 2. Application to data for rocks, sediments, and soils. Journal of Geophysical Research, 107, 1-15.

Evans, M.E., Heller, F., 2003. Environmental Magnetism. Principles and Applications of Enviromagnetics. San Diego (United States), Elsevier Sciences, Academic Press, 299pp.

Eybergen, F.A., Imeson, A.C., 1989. Geomorphological processes and climatic change. Catena, 16, 307-319.

Fang, X.-M, Ono, Y., Fukusawa, H., Bao-Tian, P., Li, J.-J., Dong-Hong, G., Oi, K., Tsukamoto, S., Torii, M., Mishima, T., 1999. Asian summer monsoon instability during the past 60,000 years: magnetic susceptibility and pedogenic evidence from the western Chinese Loess Plateau. Earth and Planetary Science Letters, 168, 219-232.

Faust, D., Zielhofer, C., Escudero, R.B., del Olmo, F.D., 2004. High-resolution fluvial record of late Holocene geomorphic change in northern Tunisia: climate or human impact? Quaternary Science Review, 23, 1757-1775.

Fenech, K., 2007. Human-induced changes in the environment and landscape of the Maltese Islands from the Neolithic to the 15th century AD. Oxford, British Archaeological Reports Limited (BAR) S1682, Archaeopress.

Fletcher, W.J., Sánchez Goñi, M.F., 2008. Orbital-and sub-orbital-scale climate impacts on vegetation of the western Mediterranean basin over the last 48,000 yr. Quaternary Research, 70, 451-464.

Fletcher, W.J., Zielhofer, C., 2013. Fragility of Western Mediterranean landscapes during Holocene rapid climate changes. Catena, 103, 16-29.

Frenzel, B., Pecsi, M., Velichko, A. 1992. Atlas of Paleoclimates and Paleoenvironments of the Northern Hemisphere, Late Pleistocene–Holocene. Budapest, Geographical Research Institute, Hungarian Academy of Sciences, and Stuttgart (Germany), Gustav Fischer Verlag, 146pp.

Giessner, K., 1990. Geo-ecological controls of fluvial morphodynamics in the Mediterranean subtropics. Geoökodynamik, 11, 17-42.

Giorgi, F., 2006. Climate change Hot-spots. Geophysical Research Letters, 33, L08707. DOI: 10.1029/2006GL025734

Giorgi, F., Lionello, P., 2008. Climate change projections for the Mediterranean region. Global and Planetary Change, 63, 90-104.

Giralt, S., Burjachs, F., Roca, J.R., Julià, R., 1999. Late Glacial to Early Holocene environmental adjustment in the Mediterranean semi-arid zone of the Salines playa-lake (Alicante, Spain). Journal of Paleolimnology, 21, 449-460.

Gómez-Paccard, M., Larrasoaña, J.C., Sancho, C., Muñoz, A., McDonald, E., Rhodes, E.J., Osácar, M.C., Costa, E., Beamud., E., 2013. Environmental response of a fragile, semiarid landscape (Bardenas Reales Natural Park, NE Spain) to Early Holocene climate variability: A paleo- and environmental-magnetic approach. Catena, 103, 30-43.

González-Sampériz, P., Valero-Garcés, B.L., Moreno, A., Jalut, G., García-Ruiz, J.M., Martí-Bono, C., Delgado-Huertas, A., Navas, A., Otto, T., Dedoubat, J.J., 2006. Climate variability in the Spanish Pyrenees during the last 30,000 yr revealed by the El Portalet sequence. Quaternary Research, 66, 38-52.

Harvey, A.M., Foster, G., Hannam, J., Mather, A.E., 2003. The Tabernas alluvial fan and lake system, southeast Spain: applications of mineral magnetic and pedogenic iron oxide analyses towards clarifying the Quaternary sediment sequences. Geomorphology, 50, 151-171.

Hogg, S.E., 1982. Sheetfloods, sheetwash, sheetflow, or...? Earth Science Reviews, 18, 59-76.

Huerta, P., Armenteros, I., 2005. Calcrete and palustrine assemblages on a distal alluvial-floodplain: A response to local subsidence (Miocene of the Duero basin, Spain). Sedimentary Geology, 177, 253-270.

Hurrel, J.W., Deser, C., 2009. North Atlantic climate variability: The role of the North Atlantic Oscillation. Journal of Marine Systems, 78, 28-41.

Jambrina, M., Rico, M., Moreno, A., Valero Garcés, B., 2011. La secuencia sedimentaria del Lago de Sanabria (Zamora, Noroeste de España). Geogaceta, 50(2), 113-116.

Juárez, M.T., Lowrie, W., Osete, M.L., Meléndez, G., 1998. Evidence of widespread Cretaceous remagnetization in the Iberian Range and its relation with the rotation of Iberia. Earth and Planetary Science Letters, 160, 729-743.

Langbein, W.B., Schumm, S.A., 1958. Yield of sediment in relation to mean annual precipitation. American Geophysical Union Transactions, 39, 1076-1084.

Lionello, P., 2012. The Climate of the Mediterranean Region. From the past to the future. Amsterdam, Elsevier, 1st Edition, 592pp. ISBN: 9780124160422

Liu, Q.S., Deng, C.L., Yu, Y.J., Torrent, J., Jackson, M.J., Banerjee, S.K., Zhu, R.X., 2005. Temperature dependence of magnetic susceptibility in an argon environment: implications for pedogenesis of Chinese loess/palaeosols. Geophysical Journal International, 161, 102-112.

Liu, Q.S., Roberts, A.P., Larrasoaña, J.C., Banerjee, S.K., Guyodo, Y., Tauxe, L., Oldfield, F., 2012. Environmental magnetism: Principles and applications. Reviews of Geophysics, 50, RG4002. DOI:10.1029/2012RG000393

Luzón, A., 2005. Oligocene–Miocene alluvial sedimentation in the northern Ebro Basin, NE Spain: Tectonic control and palaeogeographical evolution. Sedimentary Geology, 177, 19-39.

Luzón, A., Pérez, A., Mayayo, M.J., Soria, A.R., Sanchez-Goñi, M.F., Roc, A.C., 2007. Holocene environmental changes in the Gallocanta lacustrine basin, Iberian Range, NE Spain. The Holocene, 17, 649-663.

Luzón, A., Pérez, A., Borrego, A.G., Mayayo, M.J., Soria, A.R., 2011. Interrelated continental sedimentary environments in the central Iberian Range (Spain): Facies characterization and main palaeoenvironmental changes during the Holocene. Sedimentary Geology, 239, 87-103.

Luzón, A., Gauthier, A., Pérez, A., Mayayo, M.J., Borrego, A., Muñoz, A., 2012. Cambios ambientales y su reflejo en la vegetación durante el Holoceno en el sector central de la Cordillera Ibérica (Cuenca del río Añamaza, NE de España). Oviedo (España), VII Congreso Geológico de España. Geotemas, 13, 242.

Macklin, M.G., Fuller, I.C., 2002. Correlation of fluvial sequences in the Mediterranean basin over the last 200 ka and their relationship to climate change. Quaternary Science Reviews, 21, 1633-1641.

Morellón, M., Valero-Garcés, B., Vegas, T., González-Sampériz, P., Romero, O., Delgado- Huertas, A., Mata, P., Moreno, A., Rico, M., Corella, J.P., 2009. Late glacial and Holocene palaeohydrology in the western Mediterranean region: the Lake Estanya record (NE Spain). Quaternary Science Reviews, 28, 2582-2599.

Moreno, A., Cacho, I., Canals, M., Prins, M.A., Sánchez-Goñi, M.F., Grimalt, J.O., Weltje, G.J., 2002. Saharan Dust Transport and High-Latitude Glacial Climatic Variability: The Alboran Sea Record. Quaternary Research, 58, 318-328.

Moreno, A., Cacho, I., Canals, M., Grimalt, J.O., Sánchez-Goñi, M.F., Shackleton, N.J., Sierro, F.J., 2005. Links between marine and atmospheric processes oscillating at millennial time-scale. A multy-proxy study of the last 50,000 yr from the Alboran Sea (Western Mediterranean Sea). Quaternary Science Reviews, 24, 1623-1636.

Moreno, A., Stoll, H., Jiménez-Sánchez, M., Cacho, I., Valero-Garcés, B., Ito, E., Edwards, R.L., 2010a. A speleothem record of glacial (25–11.6 kyr BP) rapid climatic changes from northern Iberian Peninsula. Global and Planetary Change, 71, 218-231.

Moreno, A., Valero-Garcés, B.L., Jiménez Sánchez, M., Domínguez, M.J., Mata, P., Navas, A., González-Sampériz, P., Stoll, H., Farias, P., Morellón, M., Corella, P., Rico, M., 2010b. The last deglaciation in the Picos de Europa National Park (Cantabrian Mountains, northern Spain). Journal of Quaternary Science, 25, 1076-1091. DOI: 10.1002/jqs.1265.

Muñoz Sobrino, C., Ramil Rego, P., Gómez Orellana, L., 2004. Vegetation in the Lago de Sanabria Area (NW Iberia) since the end of the Pleistocene: a palaeoecological reconstruction

on the basis of two new pollen sequences. Vegetation History and Archaeobotany, 13, 1-22.

Ortiz, J.E., Torres, T., Delgado, A., Llamas, F.J., Soler, V., Valle, M., Julià, R., Moreno, L., Díaz-Bautista, A., 2010. Palaeoenvironmental changes in the Padul Basin (Granada, Spain) over the last 1Ma based on the biomarker content. Palaeogeography, Palaeoclimatology, Palaeoecology, 298, 286-299.

Paillard, D., Labeyrie, L., Yiou, P., 1996. Macintosh program performs time-series analysis. Eos Transactions, American Geophysical Union, 77, 379.

Peñalba, M.C., Arnold, M., Guiot, J., Duplessy, J.C., de Beaulieu, J.L., 1997. Termination of the Last Glaciation in the Iberian Peninsula inferred from the Pollen sequence of Quintanar de la Sierra. Quaternary Research, 48, 205-214.

Pérez-Obiol, R., Julià, R., 1994. Climate change on the Iberian Peninsula recorded in a 30,000yr pollen record from Lake Banyoles. Quaternary Research, 41, 91-98.

Pérez-Obiol, R., Jalut, G., Julià, R., Pèlachs, A., Iriarte, M.J., Otto, T., Hernández-Beloqui, B., 2010. Mid-Holocene vegetation and climatic history of the Iberian Peninsula. The Holocene, 21(1), 75-93. DOI:10.1177/0959683610384161

Peters, D., Dekkers, M.J., 2003. Selected room temperature magnetic parameters as a function of mineralogy, concentration and grain size. Physics and Chemistry of the Earth, 28, 659-667.

Pla Pueyo, S., Gierlowski-Kordesch, E.H., Viseras, C., Soria, J.M., 2009. Major controls on carbonate deposition during the evolution of a continental basin: Pliocene-Pleistocene of the Guadix Basin (Betic Cordillera, southern Spain). Sedimentary Geology, 219, 97-114.

Pope, R.J.J., Millington, A.C., 2000. Unravelling the patterns of alluvial fan development using mineral magnetic analysis: examples from the Sparta Basin, Lakonia, southern Greece. Earth Surface Processes and Landforms, 25, 601-615.

Pope, R.J.J., Wilkinson, K.N., 2005. Reconciling the roles of climate and tectonics in Late Quaternary fan development on the Spartan piedmont, Greece. In: Harvey, A.M., Mather, A.E., Stokes, M. (eds.). Alluvial Fans: Geomorphology, Sedimentology, Dynamics. Geological Society, 251 (Special Publications), 133-152.

Pope, R.J.J., Wilkinson, K.N., Millington., A.C,. 2003. Human and Climatic Impact on Late Quaternary Deposition in the Sparta Basin Piedmont: Evidence from Alluvial Fan Systems. Geoarchaeology, 18, 685-724.

Pope, R.J.J., Wilkinson, K., Skourtsos, E., Triantaphyllou, M., Ferrier, G., 2008. Clarifying stages of alluvial fan evolution along the Sfakian piedmont, southern Crete: New evidence from analysis of post-incisive soils and OSL dating. Geomorphology, 94, 206-225.

Rasmussen, S.O., Seierstad, I.K., Andersen, K.K., Bigler, M., Dahl-Jensen, D., Johnsen, S.J., 2008. Synchronization of the NGRIP, GRIP, and GISP2 ice cores across MIS 2 and palaeoclimatic implications. Quaternary Science Reviews, 27, 18-28.

Reimer, P.J., Baillie, M.G.L., Bard, E., Bayliss, A., Beck, J.W., Blackwell, P.G., Bronk Ramsey, C., Buck, C.E., Burr, G.S., Edwards, R.L., Friedrich, M., Grootes, P.M., Guilderson, T.P., Hajdas, I., Heaton, T.J., Hogg, A.G., Hughen, K.A., Kaiser, K.F., Kromer, B., McCormac, F.G., Manning, S.W., Reimer, R.W., Richards, D.A., Southon, J.R., Talamo, S., Turney, C.S.M., Van Der Plicht, J., Weyhenmeyer, C.E., 2009. IntCal09 and Marine09 radiocarbon age calibration curves, 0–50,000 cal years BP. Radiocarbon, 51(4), 1111-1150.

Rohdenburg, H., 1989. Landscape ecology, geomorphology. Reiskirchen (Germany), Catena, 177pp.

Rowe, P.J., Maher, B.A., 2000. Cold stage formation of calcrete nodules in the Chinese Loess Plateau: evidence from U-series dating and stable isotope analysis. Palaeogeography, Palaeoclimatology, Palaeoecology, 157, 109-125.

Sanchez-Goñi, M.F., Cacho, I., Turon, J.L., Guiot, J., Sierro, F.J., Peypouquet, J.P., Grimalt, J., Shackleton, N.J., 2002. Synchroneity between marine and terrestrial responses to millenial scale climatic variability during the last glacial period in the Mediterranean region. Climate Dynamics, 19, 95-105.

Sancho, C., Peña, J.L., Muñoz, A., Benito, G., McDonald, E., Rhodes, E.J., Longares, L.A., 2008. Holocene alluvial morphopedosedimentary record and environmental changes in the Bardenas Reales Natural Park (NE Spain). Catena, 73, 225-238.

Schnurrenberger, D., Russell, J., Kelts, K., 2003. Classification of lacustrine sediments based on sedimentary components. Journal of Paleolimnology, 29, 141-154.

Schulte, L., 2002. Climatic and human influence on river systems and glacier fluctuations in southeast Spain. Quaternary International, 93-94, 85-100.

Schulte, L., Julià, R., Burjachs, F, Hilgers, A., 2008. Middle Pleistocene to Holocene geochronology of the River Aguas terrace sequence (Iberian Peninsula): Fluvial response to Mediterranean environmental change. Geomorphology, 98, 13-33.

Schulte, L., Peña, J. C., Carvalho, F., Schmidt, T., Julià, R., Llorca, J., Veit, H., 2015. A 2600 year history of floods in the Bernese Alps, Switzerland: frequencies, mechanisms and climate forcing. Hydrology and Earth System Sciences, 12, 3391-3448. DOI:10.5194/hessd-12-3391-2015.

Thompson, R., Oldfield, F., 1986. Environmental Magnetism. London, George Allen and Unwin, 227pp.

Thorndycraft, V.R., Benito, G., 2006. The Holocene fluvial chronology of Spain: evidence from a newly compiled radiocarbon database. Quaternary Science Reviews, 25, 223-234.

Uribelarrea, D., Benito, G., 2008. Fluvial changes of the Guadalquivir river during the Holocene in Córdoba (Southern Spain). Geomorphology, 100, 14-31.

Valero-Garcés, B.L., Moreno, A., 2011. Iberian lacustrine sediment records: responses to past and recent global changes

in the Mediterranean region. Journal of Paleolimnology, 46, 319-325.

Valero-Garcés, B.L., Zeroual, E., Kelts, K., 1998. Arid phases in the western Mediterranean region during the last glacial cycle reconstructed from lacustrine records. In: Benito, G., Baker, V.R., Gregory, K.J. (eds.). Paleohydrology and Environmental Change, 67-80.

Valero-Garcés, B.L., Martí, C., García-Ruiz, J.M., González-Sampériz, P., Lorente, A., Begueira S., Navas, A., Machín, J., Delgado-Huertas, A., Stevenson, T., Basil, D., 2001. Lateglacial and early holocene paleohydrological and environmental change along a humid-arid transect from the Central Pyrenees to the Ebro Valley (Spain). Terra Nostra, 3, 211-218.

Vásquez-Méndez, R., Ventura-Ramos, E., Oleschko, K., Hernández-Sandoval, L., Parrot, J.F., Nearing, M.A., 2010. Soil erosion and runoff in different vegetation patches from semiarid Central Mexico. Catena, 80, 162-169.

Verosub, K.L., Roberts, A.P., 1995, Environmental magnetism: past, present and future. Journal of Geophysical Research, 100, 2175-2192.

Viles, H.A., Goudie, A.S., 2003. Interannual, decadal and multidecadal scale climatic variability and geomorphology. Earth-Science Reviews, 61, 105-131.

Villalaín, J.J., Fernández-González, G., Casas, A.M., Gil-Imaz., V, 2003. Evidence of a Cretaceous remagnetization in the Cameros Basin (North Spain): implications for basin geometry. Tectonophysics, 377, 101-117.

Visher, G.S., 1969. Grain size distributions and depositional processes. Journal of Sedimentary Petrology, 39, 1074-1106.

Waters, M.R., Haynes, C.V., 2001. Late Quaternary arroyo formation and climate change in the American Southwest. Geology, 29, 399-402.

White, K., Walden, J., 1997. The rate of iron oxide enrichment in arid zone alluvial fan soils, Tunisian Southern Atlas, measured by mineral magnetic techniques. Catena, 30, 215-227.

White, K., Drake, N., Millington, A., Stokes, S., 1996. Constraining the timing of alluvial fan response to Late Quaternary climatic changes, southern Tunisia. Geomorphology, 17, 295-304.

Worm, H.U., 1998. On the superparamagnetic-stable single domain transition for magnetite, and frequency dependence of susceptibility. Geophysical Journal International, 133, 201-206.

Zielhofer, C., Faust, D., 2008. Mid- and Late Holocene fluvial chronology of Tunisia. Quaternary Science Reviews, 27, 580-588.

Manuscript received June 2015;
revision accepted December 2015;
published Online May 2016.